Extended One-Dimensional Supramolecular Assembly on a Stepped Surface

J. Schnadt,[1] E. Rauls,[1] W. Xu,[1] R. T. Vang,[1] J. Knudsen,[1] E. Lægsgaard,[1] Z. Li,[2] B. Hammer,[1] and F. Besenbacher[1,*]

[1]*Interdisciplinary Nanoscience Center (iNANO) and Department of Physics and Astronomy, University of Aarhus, Building 1521, Ny Munkegade, 8000 Aarhus C, Denmark*

[2]*Institute for Storage Ring Facilities at the University of Aarhus (ISA), Building 1525, Ny Munkegade, 8000 Aarhus C, Denmark*

(Received 24 August 2007; published 30 January 2008)

2,6-naphthalene-dicarboxylic acid was adsorbed on a Ag(110) surface with an average terrace width of only some tens of a nm. Scanning tunneling microscopy shows that the adsorbates self-assemble into one-dimensional mesoscale length chains. These extend over several hundred nanometers and thus the structure exhibits an unprecedented tolerance to monatomic surface steps. Density functional theory and x-ray photoelectron spectroscopy explain the behavior by a strong intermolecular hydrogen bond plus a distinct template-mediated directionality and a high degree of molecular backbone flexibility.

DOI: 10.1103/PhysRevLett.100.046103 PACS numbers: 68.43.Bc, 68.37.Ef, 68.43.Hn

It is well known that organic molecules can self-assemble on surfaces through hydrogen-bond formation [1,2]. Self-assembly, besides being of fundamental scientific interest in itself, is thought to be a viable pathway towards functional supramolecular architectures in nanotechnology. One challenge in the field is to design self-assembled structures which are insensitive to native surface defects. As an example, on perfect surfaces the formation of one-dimensional (1D) structures can be controlled relatively easily [1], while on surfaces with many structural defects such as step edges the formation of 1D structures represents a much greater challenge. The defects can hinder the mesoscopic-scale ordering of the molecular building blocks and make a proper functioning of the assembly impossible. Here we show how hydrogen bonding of organic molecules on a stepped metal surface leads to linear self-assembled structures, ''1D chains'', that extend into the mesoscale length regime. The system is tolerant to monoatomic step edges.

The 1D chains, formed upon adsorption of submonolayer (ML) amounts of 2,6-naphthalene-dicarboxylic acid [NDCA, $C_{10}H_6(COOH)_2$] on a stepped Ag(110) single crystal surface, were characterized by scanning tunneling microscopy (STM) and x-ray photoelectron spectroscopy (XPS). STM was performed on an ultrahigh vacuum Aarhus STM [3], and XPS was carried out at the SX-700 beam line of the synchrotron radiation facility ASTRID in Aarhus, Denmark (see [4] for experimental details). Density-functional theory (DFT) calculations were carried out using the plane wave-based DACAPO package [5].

The large-scale STM topograph in Fig. 1(a) reveals that the NDCA self-assembly on Ag(110) results in close-to-straight 1D chains in the $[\bar{1}10]$ direction, which extend on the mesoscale length regime in spite of the stepped character of the surface. An analysis of the STM image yields a lower limit to the average 1D chain length of about 0.14 μm. This is a lower limit since $\sim$50% of all 1D chains extend into the surrounding area not imaged. The longest 1D chain is at least 0.65 μm long. Owing to their large size, more than 90% of all 1D chains cross at least one step edge; the average number of steps crossed by a single 1D chain is 2.3 and the highest is 13. 24% of the 1D chains end at the steps. Comparing this to an estimated 5% or less of the total area belonging to the step edges (counting the atoms adjacent to the edge on the terraces) shows that the steps constitute a barrier for the molecular 1D chains. Nevertheless, since the large majority of all 1D chains cross one or more step edges, the continuation of the 1D chains over the step edges is energetically more favorable than the formation of open 1D chains that terminate at the steps.

Figures 1(b) and 1(c) are STM images of parts of 1D chains on flat terrace regions of the surface. Each bright protrusion in the 1D chains corresponds to one single NDCA molecule. There exist two distinct orientations of the adsorbates, either aligned with $[\bar{1}10]$ (species *A*) or slightly tilted with respect to $[\bar{1}10]$ (species *B*). Both *A* and *B* bind to neighboring molecules along $[\bar{1}10]$ in a head-to-head fashion. An analysis of a large number of STM images shows that $\sim 2/3$ of all molecules adsorb as species *A* and $\sim 1/3$ as species *B*. In Fig. 1(c) an accidental tip change resulted in an STM image with atomic resolution on an uncovered part of Ag(110) and imaging of the NDCA molecules on a covered part. From this image the location of the substrate close-packed rows within the 1D chains (white lines) and the adsorbate-substrate registry can be determined (the black lines indicate two periods of four Ag atoms each). From a detailed analysis of this and many other STM images—without tip change and atomic resolution, but with simultaneous resolution of the molecules and the substrate close-packed rows—we find that species *A* is adsorbed with the molecular axis aligned with and centered over the substrate trough. Along [001], i.e., perpendicular to the 1D chains, we find a minimum distance between any two adsorbates of two Ag atomic rows. Species *B*, in contrast, is rotated by an angle of about 40° to $[\bar{1}10]$ and positioned with its center on top of the substrate rows. Finally, Fig. 1(d) presents an STM image of a 1D

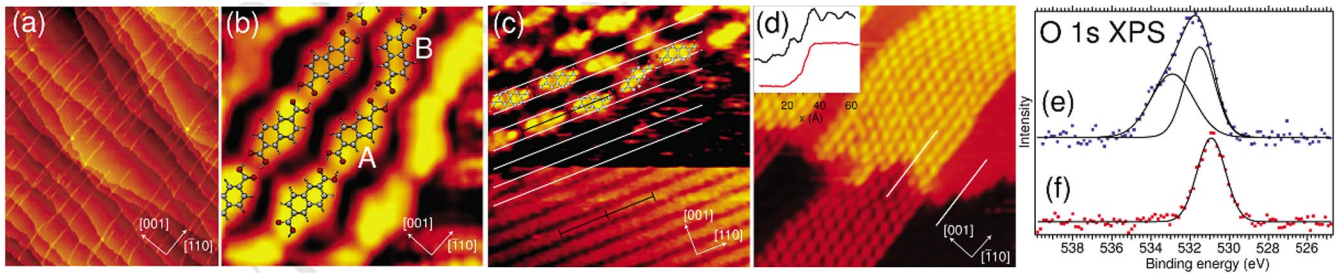

FIG. 1 (color online). STM and XPS results. (a) 620×700 Å^2, $I = -0.39$ nA, $V = -220.9$ mV, 0.1 ML NDCA/Ag(110). (b) 35×35 Å^2, -0.25 nA, -185.8 mV, ~ 0.75 ML. The molecular model stems from the optimization of a gas phase network (see text). (c) 60×60 Å^2, -0.79 nA, -883.8 mV, ~ 0.3 ML. (d) 195×195 Å^2, -0.204 nA, -262.8 mV, ~ 0.45 ML. The lines indicate the traces of the line scans in the inset. Inset: line scan over an adsorbate-covered step edge (black) and a free step edge (red). The relative alignment of the scans is arbitrary. (e), (f) O 1s XPS, (e) ~ 0.3 ML NDCA deposited onto Ag(110) at room temperature and not treated any further, (f) 1 ML NDCA deposited onto a room temperature Ag(110) surface and annealed to 200 °C for 20 min.

chain extending across a step edge. The inserted line scan with a regular structure in the NDCA protrusions across the step edge suggests that the bonding in the 1D chains is largely unaffected by the monatomic step and that the molecules on the lower terraces do not lie flat at the steps.

The O 1s XPS results in Fig. 1(e) reveal a broad peak with two components of equal weight. This spectrum was obtained on NDCA sublimated onto a room temperature Ag(110) surface and not further treated, and thus the results directly correspond to the STM measurements of Fig. 1(a)–1(d). The two components stem from the two distinct oxygen species of the protonated carboxylic group [6]. The larger width of the high binding energy as compared to the low binding energy peak is suggested to be related to the effect of intermolecular hydrogen bonding. Important here is that both components exist and that they have the same spectral weight. This proves that the carboxylic groups are protonated and that the molecules thus cannot form a covalent bond to the Ag substrate. However, owing to the XPS detection limit, the statement is valid only for the majority of molecules, i.e., for the terrace-bonded NDCAs, while a deprotonation of the step-bonded NDCA cannot be excluded so far. DFT will allow us to discard this possibility as described below. After annealing to 200 °C only one O 1s XPS peak persists [Fig. 1(f)]. This shows that all oxygen atoms have become chemically equivalent due to deprotonation and formation of a bidentate bond of the carboxylic group to the substrate. Hence, under the room temperature conditions of the STM experiments a kinetic barrier hinders the deprotonation of the NDCA.

We probed a large number of adsorbate geometries using DFT. The outcome for some of these is summarized in Table I. It should be noted that for the smallest surface unit cells the calculations were performed using two as well as three or four atomic layer slabs of Ag(110), while the systems with large surface unit cells with several NDCAs only could be modeled using two-layer Ag(110) slabs. The accuracy of the two-layer-slab results can be estimated from noting that the binding energy of NDCA in an infinite 1D chain on a Ag(110) terrace only changes from 1.20 to 1.41 eV (Table I, row 3) when going from the four-layer to the two-layer slab. Thus, the use of two-layer-slab results in our discussion is justified, in particular, since our conclusions are based on the comparison of relative energies obtained in the thin slab calculations. The DFT calculations for the adsorbate geometries at step edges were performed using an NDCA dimer, which made it possible to calculate many different NDCA geometries using a single choice of super cell without the restriction of having to choose an adsorbate cell commensurate with the substrate unit cell. Here we assume that the NDCA-NDCA and NDCA-Ag bond energies within the dimer are unaffected by the absence of the bonds between the dimer and the rest of the 1D chain. This assumption is justified by the finding of a less than 10% increase of the NDCA-NDCA bond strength when moving from the adsorbed 1D chain to the adsorbed dimer. Finally, it is noted that DFT, as well known, does not properly account for the dispersion contribution to the binding energy. From a comparison of the binding energies of benzene to Cu(111) and Cu(110) obtained from DFT to those obtained from Møller-Plesset second-order perturbation theory and/or to experiment, the here used PW91 parametrization can be expected to describe approximately 5% to 25% of the dispersion strength only [8]. However, since (a) the binding energy of the investigated systems is dominated by hydrogen bonding with an interaction strength larger than the dispersion interaction strength and (b) the dispersion interaction strength should be similar in all investigated systems, this deficiency does not invalidate our findings.

Figure 2(a) (cf. Table I, rows 3 and 4) shows the two most favorable noncovalently bonded NDCA geometries on a Ag(110) terrace. In the calculation the formation of the hydrogen bond was achieved by restricting the unit cell to single molecule on a Ag(110) slab with suitable periodic boundary conditions. In accordance with the experimental observation of species A, the geometry of Fig. 2(a) (left)

TABLE I. DFT binding energies per molecule of the indicated systems. The P (D) label refers to the protonated (deprotonated) state of the adsorbate, half-D to deprotonation of only one of the two molecular carboxylic groups. The monomer labels refer to true monomer calculations in rows 1–2 (using periodic boundary conditions on a large substrate slab), to covalently bonded NDCAs on a commensurate substrate slab in rows 6–7 [7], and to two adsorbates without hydrogen-bond interaction in a dimer calculation in rows 10, 12, and 13. The specification of the orientation refers to the direction of the molecular principal axis. The slab specification refers to the number of substrate layers in the calculation.

No.		Molecular geometry		Figure	2 layer slab	3 layer slab	4 layer slab
1	monomer	P	$\parallel [\bar{1}10]$, on top of troughs		0.31 eV		0.29 eV
2	monomer	P	$\parallel [\bar{1}10]$, on top of atomic rows		0.18 eV		0.17 eV
3	1D chain	P	$\parallel [\bar{1}10]$, on top of troughs	2(a) (left)	1.41 eV		1.20 eV
4	1D chain	P	$\parallel [\bar{1}10]$, on top of atomic rows	2(a) (right)	1.20 eV		1.09 eV
5	1D chain	P	$\perp [\bar{1}10]$				0.70 eV
6	monomer	D	covalently bonded, $\parallel [\bar{1}10]$		5.11 eV	4.65 eV	
7	monomer	D	covalently bonded, $\perp [\bar{1}10]$		5.31 eV	4.94 eV	
8	dimer	P	$\parallel [\bar{1}10]$, on top of troughs		0.91 eV		
9	dimer	P	at step edge	2(c)	0.77 eV		
10	two monomers	P	at step edge	2(d)	0.40 eV		
11	dimer	P	center of molecule on top of step edge		0.50 eV		
12	two monomers	half-D	covalently bonded to step edge	2(e)	2.70 eV		
13	two monomers	half-D	covalently bonded to step edge	2(f)	2.81 eV		
14	gas phase net	P	ratio species A:species B = 3:1	2(b)	no substrate: 0.61 eV		

with the molecules aligned over the Ag close-packed troughs is most stable. From a comparison of the chain configuration (row 3 in Table I) with an isolated NDCA monomer (row 1) it is seen that the strength of the NDCA-NDCA double bond in the infinite 1D chain amounts to (binding energy of one NDCA in the 1D chain − binding energy of an isolated NDCA) = $(1.20 - 0.29) \approx 0.9$ eV (1.1 eV on two-layer slabs), much more than the molecular bonding contribution along [001], which we have calculated to be less than 0.1 eV/NDCA [9]. The NDCA-NDCA double hydrogen-bond strength is a bit higher in the terrace-adsorbed dimer (row 8), $2 \times (0.91 - 0.31) = 1.20$ eV, where the factor 2 accounts for the fact that a dimer only contains half an intermolecular bond/NDCA. Nevertheless, a comparison of rows 3 and 8 of Table I shows clearly that the formation of 1D chains is more favorable than the formation of open-ended dimers.

Adsorbed 1D chains containing species *B* could not be modeled due to the large size of the adsorbate or substrate unit cell. Instead a gas phase net containing both species *A* and *B* in the absence of the Ag support was optimized [Fig. 2(b) and row 14 in Table I]. The resulting single molecule geometries were further optimized in the presence of the Ag(110) substrate and turned out to be equally stable. Thus, the observed 2/3:1/3 ratio of species *A* and *B* results from intermolecular interactions—in particular, along $[\bar{1}10]$—with a small energetic advantage for species *A*.

The most stable geometry of an NDCA dimer at a Ag step edge found here is characterized by an intact intermolecular hydrogen bond; cf. Figure 2(c) and row 9 of Table I. A breaking of the hydrogen bond reduces the binding energy by nearly 0.4 eV/NDCA [Fig. 2(d), row 10]. Thus theory, as experiment, invokes a notion of the lower terrace adsorbates bending up at the step edges to form head-to-head hydrogen bonds to upper terrace adsorbates. The slight bend of these molecules leads to a minor energy loss, which can be assessed from a calculation of the energy variation with molecule bending (not shown), and which is less than 0.1 eV/NDCA. It is overcompensated by the energy gain from hydrogen-bond formation across the step. Nevertheless, in line with the experimental results it is also found that the Ag step edge partially prohibits the formation of the ideal NDCA-NDCA bond. This is seen from the strengths of the hydrogen bonds at the step edges, which can be estimated to lie in between $2 \times (0.77 - 0.31) = 0.92$ eV and $2 \times (0.77 - 0.40) = 0.74$ eV. Here the reference point is either an isolated NDCA adsorbed on a terrace (row 1) or a dimer without hydrogen bond at a step edge (row 10). This value is clearly smaller than the 1.20 eV reported above for the terrace NDCA-NDCA bond.

DFT gives large binding energies for deprotonated and covalently bonded molecules at a Ag step edge [7]; cf. Fig. 2(e) and 2(f), rows 12–13 in Table I. However, a separation of the molecules parallel to the step edge [Fig. 2(f)] is preferred over a continuation of a 1D chain over the step [Fig. 2(e)]. Thus for covalently bonded 1D chains one would expect randomly distributed 1D chains which end at the step edges, at variance with the experimental finding of unbroken 1D chains across the steps. Hence our assumption that all adsorbates are fully protonated and purely noncovalently bonded is confirmed.

Thus, we have shown that even on defect-afflicted surfaces self-assembly by hydrogen bonding can be used to build 1D macroscale structures from single molecules. The

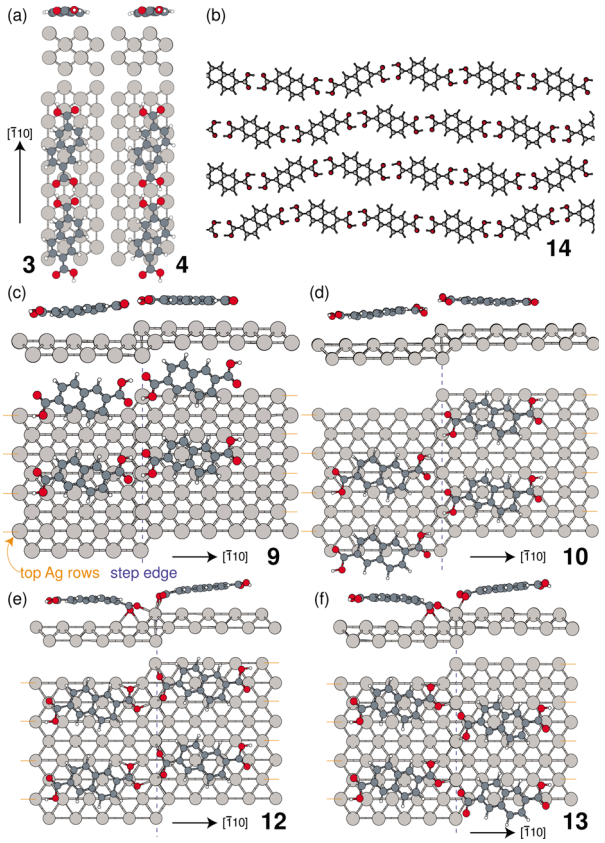

FIG. 2 (color online). DFT results. The numbers refer to Table I. (a) Head-to-head hydrogen-bonded NDCA on top of a substrate trough (left) and a close-packed Ag row (right). (b) Gas phase net of two species *A* and *B* with different orientations corresponding to the adsorbate orientations observed experimentally. (c)–(f) NDCA dimers at a step edge. (c) Most stable configuration of a protonated NDCA dimer at a step edge. (d) Two protonated NDCA without NDCA-NDCA hydrogen bonds. (e) Two deprotonated NDCA molecules in registry cross the step edge. (f) Two deprotonated NDCA molecules out of registry across the step edge.

theoretical analysis shows that the primary key factor is a robust hydrogen bond. But self-assembly across step edges also depends crucially on the directionality mediated by the substrate, since the 1D chains would not cross the step edges if there existed adsorbate geometries rotated away from the close-packed rows with energies not much smaller than those of the most stable terrace geometries. Also the energy loss inflicted by the bending of the molecules at the step edges is smaller than that for the alternative geometry of open 1D chain ends. Thus, the flexibility of the molecular structure is an additional important ingredient needed for achieving the observed monatomic step tolerance.

Roberto Otero is acknowledged for discussions. J. S. acknowledges a Marie Curie Intra-European Fellowship by the European Commission and E. R. thanks the Alexander von Humboldt-Stiftung for financial support.

*fbe@inano.dk

[1] J. V. Barth *et al.*, Angew. Chem., Int. Ed. **39**, 1230 (2000); T. Yokoyama *et al.*, Nature (London) **413**, 619 (2001); D. L. Keeling *et al.*, Nano Lett. **3**, 9 (2003); J. Weckesser *et al.*, Phys. Rev. Lett. **87**, 096101 (2001); J. V. Barth *et al.*, Appl. Phys. A **76**, 645 (2003); A. Schiffrin *et al.*, Proc. Natl. Acad. Sci. U.S.A. **104**, 5279 (2007).

[2] A. Dmitriev *et al.*, J. Phys. Chem. B **106**, 6907 (2002); S. Griessl *et al.*, Single Mol. **3**, 25 (2002); S. De Feyter *et al.*, Nano Lett. **3**, 1485 (2003); M. Lackinger *et al.*, J. Phys. Chem. B **108**, 13 652 (2004); S. Clair *et al.*, J. Phys. Chem. B **108**, 14 585 (2004); M. Lackinger *et al.*, Small **1**, 532 (2005); J. A. Theobald *et al.*, Nature (London) **424**, 1029 (2003); J. C. Swarbrick *et al.*, J. Phys. Chem. B **109**, 12 167 (2005); R. Otero *et al.*, Angew. Chem., Int. Ed. **44**, 2270 (2005); S. De Feyter *et al.*, Nano Lett. **5**, 77 (2005); G. Pawin *et al.*, Science **313**, 961 (2006); M. E. Cañas-Ventura *et al.*, Angew. Chem., Int. Ed. **46**, 1814 (2007); S. Xu *et al.*, Nano Lett. **6**, 1434 (2006); B. Xu *et al.*, J. Am. Chem. Soc. **128**, 8493 (2006); H. Li *et al.*, J. Phys. Chem. C **111**, 2102 (2007); N. Zhu, T. Osada, and T. Komeda, Surf. Sci. **601**, 1789 (2007).

[3] F. Besenbacher, Rep. Prog. Phys. **59**, 1737 (1996).

[4] The sample was cleaned using cycles of 600 eV Ar^+/Ne^+ sputtering and annealing to 480 °C. Sub-ML amounts of NDCA were sublimated onto the room temperature sample from a thermal sublimator at ~260 °C. STM imaging was facilitated by cooling to in between −100 and −170 °C. Room temperature imaging gave identical results, but one had to be more careful in order not to destroy the assembly due to the tip-adsorbate interaction.

[5] B. Hammer, L. B. Hansen, and J. K. Nørskov, Phys. Rev. B **59**, 7413 (1999); S. R. Bahn and K. W. Jacobsen, Comput. Sci. Eng. **4**, 56 (2002).

[6] L. Patthey *et al.*, J. Chem. Phys. **110**, 5913 (1999); A. Dmitriev *et al.*, Chem. Phys. Chem. **7**, 2197 (2006).

[7] For the deprotonated and covalently bonded molecules the H atoms are assumed to end up in H_2 at 0 K.

[8] A. Bilić *et al.*, J. Chem. Theory Comput. **2**, 1093 (2006); P. S. Bagus, K. Hermann, and C. Wöll, J. Chem. Phys. **123**, 184109 (2005).

[9] In this calculation the DACAPO code was extended with a London-type dispersion term.